Journal of Ceramic Processing Research. Vol. 12, No. 5, pp. 525~529 (2011)

J O U R N A L O F
Ceramic Processing Research

Thermal conductivity of micro hot-pressed AlN ceramics fabricated using a conventional $MoSi_2$ heating element furnace

Chih-Peng Lin[a,*], Chih-Hung Chu[b], Shaw-Bing Wen[c] and Yun-Hwei Shen[b]

[a]*Department of Leisure and Recreation Management, Diwan College of Management, Tainan 721, Taiwan*
[b]*Department of Resources Engineering, National Cheng Kung University, Tainan 701, Taiwan*
[c]*General Education Center, Meiho Institute of Technology, Neipu, Pingtung 912, Taiwan*

AlN samples doped with sub-micron Y_2O_3 and CaO powders as sintering additives obtained using the micro hot-pressed (MHPed) sintering method in a $MoSi_2$ heating element furnace were investigated. The minor amounts of secondary phases were identified as $Al_5Y_3O_{12}$, $CaYAl_3O_7$, and $CaAl_4O_7$, which are related to the low sintering temperature as well as the removal of oxygen-related defects in the system. Relative densities of over 96% of the theoretical value were obtained after sintering at 1600 °C for 8 h, indicating that an adequate amount of additives and the use of the micro hot-pressed (MHPed) sintering process help improve the densification and thermal conductivity of AlN ceramics. The high thermal conductivity of 130 $Wm^{-1}K^{-1}$ was attributed to the purification of the AlN lattice, the elimination of some secondary phases, and the grain boundary phase distribution.

Key words: Aluminum nitride, Sub-micron, Micro hot-pressed, Thermal conductivity, $MoSi_2$ heating element.

Introduction

Aluminum nitride (AlN) is considered a promising substrate and packaging material for high power integrated circuits because of its high thermal conductivity, low dielectric constant, a thermal expansion coefficient close to that of silicon and high electrical resistivity [1-3]. However, due to its high covalent bonding, it is difficult to achieve solid-state sintering without using sub-micron powders or a high pressure [2]. Liquid-phase sintering can be carried out to produce densified AlN ceramics. The most common additives are rare-earth and/or alkaline earth oxides [4, 5], which react with Al_2O_3 on the surface of AlN powders during sintering. Recently, there has been a growing interest in the low-temperature sintering of AlN bulk material, which reduces manufacturing costs [6-8].

The authors previously reported that AlN ceramics with Y_2O_3 and CaO can be densified using an alumina (Al_2O_3) crucible and a conventional $MoSi_2$ heating element furnace, thus avoiding the requirement of using a controlled atmosphere in a furnace [9]. High-pressure sintering has been regarded as an effective method for lowering the sintering temperature and improving the driving force. Li *et al*. [10] found that the relative density of AlN bulk material with 5 wt.% La_2O_3 addition sintered at 1300 °C and 5.0 GPa for 50 minutes was 96.3%. A high density of over 99% was obtained when the temperature was increased from 1300 °C to 1600 °C. It is noted that hot-pressed (HP) sintering of ceramic materials at high or micro pressure is rarely applied in studies of AlN bodies.

The purpose of this study is to modify the conventional procedure to allow the densification of AlN to be carried out using the micro hot-pressed (MHPed) sintering technique. The densification can be conducted using an alumina (Al_2O_3) crucible and a piston in a $MoSi_2$ heating element furnace at 1600 °C for 8 h with a conventional flow of nitrogen. The effects of densification, lattice purification, phase composition, and grain boundary phases on the thermal conductivity of the micro hot-pressed (MHPed) sintered AlN doped with Y_2O_3 and CaO are investigated.

Experimental Procedure

Commercially available AlN powder (Grace Derwey Co., Ltd. Agency) with a particle size (D_{50}) of 1.92 μm and an oxygen impurity content of 1.0 wt.% was used as the feedstock. Y_2O_3 (Alfa Aesar, purity 99.9%, D_{50}: 7.23 μm) and CaO were selected as sintering additives. CaO powder was added as $CaCO_3$ (J. T. Baker, purity 99.8%, D_{50} : 16.38 μm). Table 1 shows the particle size distributions of the raw additives before and after ball milling for 48 h.

Table 1. Particle size distributions of raw additives before and after ball milling for 48 h

Additives	Ball milling	D_{10} (μm)	D_{50} (μm)	D_{90} (μm)
$CaCO_3$	Before	2.05	20.71	36.47
	after	0.26	0.48	1.31
Y_2O_3	Before	1.73	7.23	32.29
	after	0.38	0.69	1.51

*Corresponding author:
Tel : +886-6-571-8888 ext 637
Fax: +886-6-571-6298
E-mail: ftirlin@gmail.com

The raw powders contained a significant proportion of particles with sizes above 6 μm. The particle size (D_{50}) decreased to less than 0.7 μm after grinding.

AlN was wet mixed with 0.215-0.86 mole% (corresponding to 1.2 wt.%-4.6 wt.%) Y_2O_3 and 0.86-2.15 mole% (corresponding to 1.2 wt.%-2.9 wt.%) CaO, respectively, using vibration milling for 5 h. The powder composition is given in Table 2. After being dried and passed through a 100-mesh sieve, the granules were uniaxially pressed at 40 MPa in a cylindrical steel die. The pellets (16.5 mm in diameter and about 1.7 mm in thickness) were then cold isostatically pressed (CIPed) under 98 MPa. The binder was then removed by heating at 450 °C for 1 h.

Fig. 1 shows a schematic representation of the arrangement of a test specimen together with the Al_2O_3 piston and crucible. The pellet, which was embedded in a boron nitride (Avocado, purity 99%) powder bed, was sandwiched by BN plates, that was placed on a base of graphite inside an Al_2O_3 crucible completely enveloped by a carbon black (Alfa Aesar, purity 99%) powder bed. Then, the samples were treated at 1600 °C for 8 h in a $MoSi_2$ heating furnace with a conventional flow of nitrogen (Yunshan Co. Ltd., purity 95%).

The apparent densities were measured using the Archimedes method. X-ray diffraction analysis (XRD, Siemens D5000) was employed to identify the phases evolved in each specimen. To determine the lattice parameters, the samples sintered at 1600 °C for 8 h were scanned in the range of 2θ from 20° to 80° at a rate of 0.02°sec^{-1} using XRD with Cu K_α radiation at 40 KV and 40 mA. Microstructures were observed using a scanning electron microscope (SEM, Hitachi TM-1000). Thermal diffusivities were measured using a laser flash thermal constant analyzer (Laser Flash LFA-447) and the thermal conductivity at room temperature was calculated from the equation $\kappa = C\upsilon d$, where C is the specific heat, υ is the thermal diffusivity, and d is the density of the sample (ASTM E1461).

Table 2. Compositions of various AlN-Y_2O_3-CaO powder mixtures

Specimen	AlN (mole%)	Y_2O_3 (mole%)	CaO (mole%)
Y0.215C1.72	98.065	0.215	1.72
Y0.43C1.72	97.850	0.43	1.72
Y0.215C2.15	97.635	0.215	2.15
Y0.43C2.15	97.420	0.43	2.15
Y0.86C0.86	98.280	0.86	0.86
Y0.86C1.29	97.850	0.86	1.29
Y0.86C1.72	97.420	0.86	1.72
Y0.86C2.15	96.990	0.86	2.15

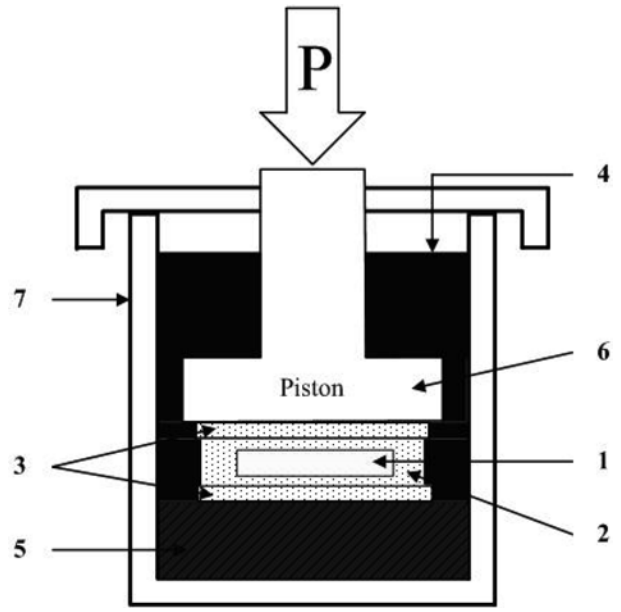

Fig. 1. Schematic representation of the arrangement of (1) test specimen with the (2 and 3) protective materials of BN, (4) carbon black, (5) a base of graphite, and (6) alumina piston placed in (7) an Al_2O_3 crucible for micro hot-pressed (MHPed) sintering.

Results and Discussion

Phase compositions of micro hot-pressed sintered AlN

Table 3 summarizes the phase compositions and amounts of various secondary phases in each specimen sintered at 9.8 kPa and 1600 °C for 8 h. At a given yttria level, the amount of $Al_5Y_3O_{12}$ decreased with an increase in the CaO/Y_2O_3 ratio, and additional secondary phases $CaYAl_3O_7$ and $CaAl_4O_7$ were identified. Since both $CaYAl_3O_7$ and $CaAl_4O_7$ phases formed at the temperature of 1600 °C, the amount of CaO significantly influenced the formation of Y-Al-O and Ca-Y-Al-O compounds due to the consumption of surface Al_2O_3 on the AlN particles. Thus, Y_2O_3 and CaO allow the formation of the grain boundary phases of $Al_5Y_3O_{12}$, $CaYAl_3O_7$, and $CaAl_4O_7$, which are related to (1) the low the sintering temperature and enhanced densification through liquid-phase sintering and to (2) the movement of oxygen atoms from both the AlN lattice and grain surfaces to the grain boundaries.

Table 3. Phase compositions and amounts of secondary phases in specimens sintered

Specimen	Secondary phases		
	$Al_5Y_3O_{12}$	$CaYAl_3O_7$	$CaAl_4O_7$
Y0.86C0.86	H	N	N
Y0.86C1.29	M	M	N
Y0.86C1.72	M	N	H
Y0.86C2.15	L	H	L
Y0.215C1.72	L	N	H
Y0.43C1.72	M	N	H
Y0.215C2.15	L	L	H
Y0.43C2.15	L	M	M

N : None, L : low, M : medium, and H : high.

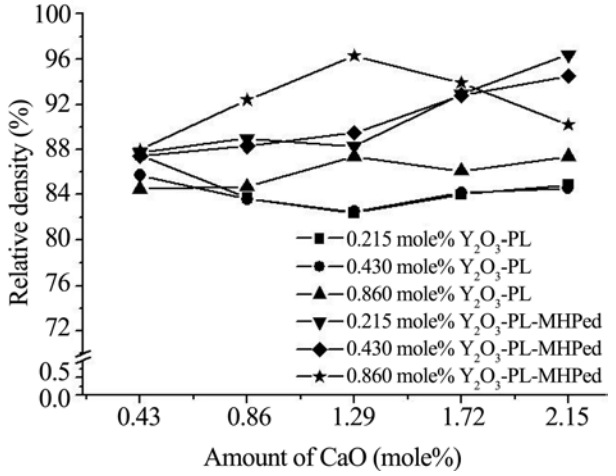

Fig. 2. Comparison of relative density for micro hot-pressed and pressure-less AlN samples with various amounts of Y_2O_3 and CaO sintered at 1600 °C for 8 h and at 9.8 kPa.

Densification of micro hot-pressed sintered AlN

Fig. 2 shows the relative density as a function of the amounts of Y_2O_3 and CaO for samples sintered at 1600 °C for 8 h. The maximum relative density of 96.4% for the AlN sample obtained using micro hot-pressed (MHPed) sintering is higher than the maximum relative density of 88% obtained for pressure-less sintered AlN. The driving force of micro hot-pressed (MHPed) sintering includes an additional compressive force, which improves the densification of sintered AlN.

The relative densities of AlN samples doped with 0.215 and 0.43 mole% Y_2O_3, respectively, increased when the CaO content was increased. In contrast, samples doped with 0.86 mole% Y_2O_3 first steeply increased and then starting at 1.29 mole% decreased with an increasing amount of CaO, achieving a maximum density of 96.3%. It is believed that high density AlN bulk materials can be prepared by adding an adequate amount of mixed additives and using micro hot-pressed (MHPed) sintering at the relatively low temperature of 1600°C. Previously, Li *et al.* [10] produced AlN ceramics doped with La_2O_3 under a high pressure of 5 GPa at a low temperature of 1300 °C, which is more than 300 °C lower than that for conventional liquid-phase sintering.

Thermal conductivity of micro hot-pressed AlN

It is well known that the density, secondary phases at grain boundaries, lattice-oxygen and defects within sintered AlN are the main factors affecting the thermal conductivity [11]. Table 4 summarizes the lattice parameters, density, and thermal conductivity of AlN samples doped with Y_2O_3 and CaO. When 1.72 mole% CaO was added, the thermal conductivity increased from 123 to 130 $Wm^{-1}K^{-1}$ and the c-axis increased in length from 4.9786 to 4.9799 Å. It is noted that the purification of the AlN lattice increases the length of the c-axis. A decrease of the length of the c-axis during sintering implies that oxygen diffuses into the AlN lattice and increases the number of defects, thus degrading the thermal conductivity [12].

Table 4. Lattice parameters, relative density and thermal conductivity of micro hot-pressed sintered AlN samples

Specimen	a (Å)	c (Å)	Unit cell volume ($Å^3$)	Relative density (%)	Thermal conductivity ($Wm^{-1}K^{-1}$)
Y0.86C0.86	3.1112	4.9782	41.731	92.4	130.6
Y0.86C1.29	3.1113	4.9797	41.746	96.3	122.1
Y0.215C1.72	3.1122	4.9799	41.772	92.9	130.1
Y0.43C1.72	3.1112	4.9786	41.734	92.8	123.2
Y0.86C1.72	3.1112	4.9787	41.735	93.9	127.5
Y0.215C2.15	3.1113	4.9793	41.743	96.4	119.2
Y0.43C2.15	3.1133	4.9831	41.828	94.5	118.5
Y0.86C2.15	3.1117	4.9806	41.765	90.2	66.7

With the addition of 2.15 mole% CaO, the improvement in thermal conductivity mainly comes from the enhancement of densification. A higher thermal conductivity of 119.2 $Wm^{-1}K^{-1}$ was achieved for the AlN material with a density of 96.4%, whose composition contained 0.215 mole% Y_2O_3 and 2.15 mole% CaO. Although the c-axis length and density of the sample with 0.86 mole% Y_2O_3 and 0.86 mole% CaO was inferior to those of the sample with 0.86 mole% Y_2O_3 and 1.29 mole% CaO, the former yielded a high thermal conductivity (over 130 $Wm^{-1}K^{-1}$). An examination of Table 4 reveals the following: (1) the thermal conductivity of samples with 1.72 mole% CaO increases with increasing length of the c-axis, giving the high degree of purification of AlN lattices and (2) the higher thermal conductivity of samples with Y_2O_3 and CaO is due to the elimination of secondary phases.

Table 5 shows the thermal conductivities obtained in several studies. Hot-pressed insulating AlN samples with thermal conductivities of up to 160 $Wm^{-1}K^{-1}$ [13-16, 17] had no apparent secondary phases. Watari *et al.* [18] reported sintered AlN with a thermal conductivity of 155 $Wm^{-1}K^{-1}$ which had only Y_2O_3 as the secondary phase. However, in the present study, the AlN product with $Y_3Al_5O_{12}$ prepared using micro hot-pressed (MHPed) sintering had a slightly lower thermal conductivity of 130 $Wm^{-1}K^{-1}$ at 1600 °C.

Microstructural development

Fig. 3 shows the scanning electron microscope (SEM) fractographs of AlN samples doped with Y_2O_3 and CaO sintered at 1600 °C for 8 h and at 9.8 kPa. Polyhedral grains were observed in the samples with 1.72 mole% CaO and various amounts of Y_2O_3, namely 0.215, 0.43, and 0.86 mole%. These grains differ from those obtained in other test runs, which had an irregular shape. Fig. 3 (h) shows that a high volume fraction of liquid decreases the viscosity of the solid-liquid-pore ensemble and decreases the capillary force during the micro hot-pressed (MHPed) sintering, resulting in shape accommodation and delayed densification. Thus, an intermediate quantity of liquid leads to optimal viscosity and capillarity effects.

Table 5. Properties of hot-pressed sintered AlN samples

Sintering conditions				Additives	Secondary phases	Properties		Ref.
Type of crucible	Powde bed	Pressure	Settings and sintering temperature			Relative density (%)	Thermal conductivity ($Wm^{-1}K^{-1}$)	
Alumina	BN	9.8 kPa	1600 °C for 8 h, $MoSi_2$ heating furnace in N_2 gas.	Y_2O_3-CaO	$Al_5Y_3O_{12}$	92.4	130.6	This study
Alumina	BN	9.8 kPa	1600 °C for 8 h, $MoSi_2$ heating furnace in N_2 gas.	Y_2O_3-CaO	$CaAl_4O_7$, $Al_5Y_3O_{12}$	92.9	130.1	This study
		5 GPa	1300 °C for 50 minutes, a graphite tube used as heater.	La_2O_3	$LaAlO_3$	96.3	n.a.	[10]
Graphite dies	BN	9.8 MPa	1800 °C for 2 h,	CaC_2	undetected	100	180	[13]
Graphite dies		39.2 MPa	1800 °C for 2 h, in a high frequency induction furnace with an atmosphere of N_2.	None	n.a.	100	n.a.	[14]
Graphite dies	BN washcoat	20 MPa	1900 °C for 1 h, in 1 atm of N_2 gas.	None	n.a.	3.2 gcm^{-3}	100	[15]
	Tantalum sheath	5 GPa	1947 °C for 15 s	None	n.a.	> 3.25 gcm^{-3}	> 160	[16]
	Carbon foil	100 MPa	2500 °C for 1 h,	Y_2O_3	Y_2O_3	3.24 gcm^{-3}	155	[18]
CaF_2 sleeve and tantalum disc	CaF_2 carbon black	6.5 GPa	2000 °C for 30 minutes, graphite as heater.	n.a.	n.a.	3.27 gcm^{-3}	190	[17]

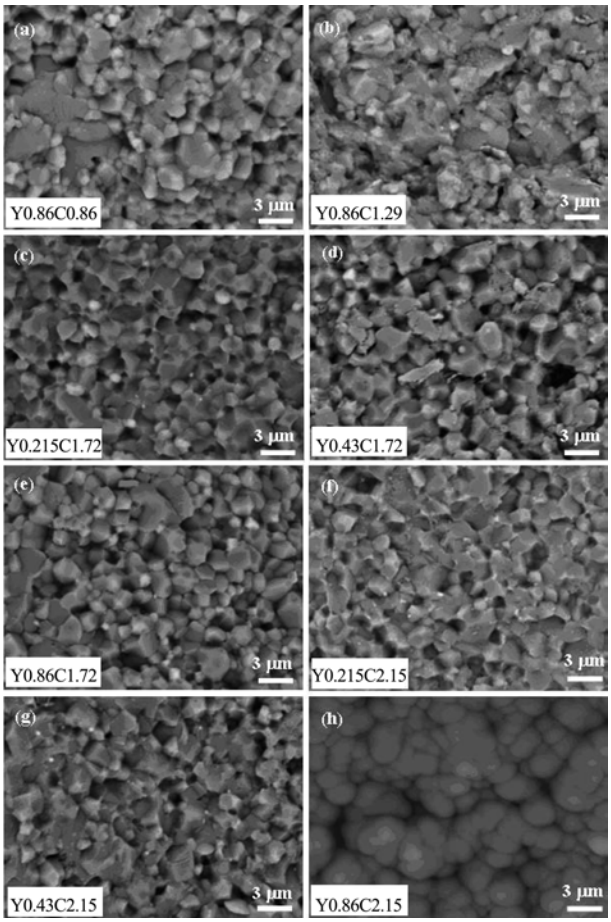

Fig. 3. SEM fractographs of micro hot-pressed sintered AlN with various amounts of Y_2O_3 and CaO fired at 1600 °C for 8 h and at 9.8 kPa.

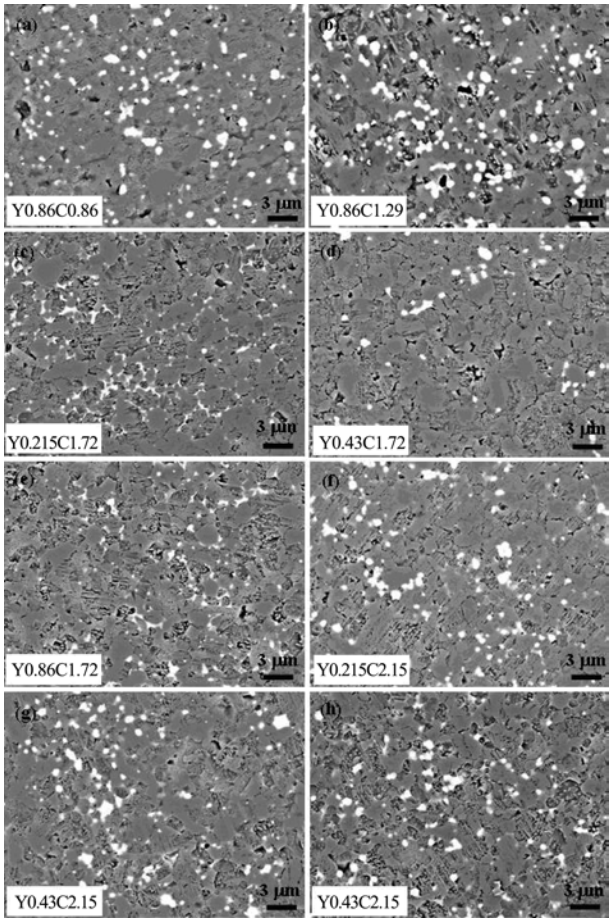

Fig. 4. SEM images of polished surface and chemical etching of samples doped with Y_2O_3 and CaO fired at 1600 °C for 8 h and at 9.8 kPa.

Fig. 4 shows the SEM photographs of the polished surfaces and chemical etching of AlN samples sintered at 1600 °C for 8 h and at 9.8 kPa. The secondary phases (bright) were primarily dispersed at the AlN grain junctions, as shown in Fig. 4(c) and (e). The effect of secondary phases is small when they are the minority phases. This helps increase the thermal conductivity since the high-thermal-conductivity AlN phase is contiguous. Beyond a certain amount, the thermal conductivity decreases because Ca-, Y-, and Ca-Y-aluminates have much lower thermal conductivities compared with that of AlN. When the secondary phases of $Al_5Y_3O_{12}$, $CaYAl_3O_7$, and $CaAl_4O_7$ isolated the AlN grains, the thermal conductivity drastically decreased, as shown in Fig. 4(b), (f), and (g). These experimental results show that the purification of the AlN lattice, the composition, and the distribution of secondary phases strongly influence the thermal conductivity of micro hot-pressed (MHPed) sintered AlN.

Conclusions

The micro hot-pressed (MHPed) sintering technique was used to obtain sintered AlN with high densities (above 96% of theoretical value). The results show that the relative densities of AlN samples with 0.215 and 0.43 mole% Y_2O_3 increased with increasing CaO additions. The relative densities of samples doped with 0.86 mole% Y_2O_3 first steeply increased, and then starting at 1.29 mole% decreased with increasing CaO additions. The Y_2O_3- to -CaO ratio is related to the formation of the minor phases of $Al_5Y_3O_{12}$, $CaYAl_3O_7$, and $CaAl_4O_7$, which are related to the low sintering temperature and the removal of the oxygen-related defects in the system. The fabrication of AlN ceramics with thermal conductivities in excess of 130 $Wm^{-1}K^{-1}$ sintered at 9.8 kPa and 1600 °C for 8 h greatly depends on $Al_5Y_3O_{12}$ as the secondary phase, the purification of the AlN lattice, and the grain boundary phase distribution.

Acknowledgements

The authors would like to thank Prof. C. S. Huang for CIPed operation, Prof. C. Y. Huang for lattice parameter calculations, and Yonyu applied technology material Co., Ltd. for measurements of thermal conductivity.

References

1. G.A. Slack, J. Phys. Chem. Solids, 34 (1973) 321-335.
2. L.M. Sheppard, Am. Ceram. Bull. 69 (1990) 1801-1812.
3. Y. Baik and R.A.L. Drew, Adv. Ceram. Materials, 122 (1996) 553-570.
4. K. Komeya, A. Tsuge and A. Inoue, J. Mater. Sci. Lett. 1 (1982) 325-326.
5. K. Komeya, H. Inoue and A. Tsuge, Yogyo-Kyokaishi, 93 (1985) 41-46.
6. K. Watari, A. Tsuzuki and Y. Torii, J. Mater. Sci. Lett. 11 (1992) 1508-1510.
7. A.V. Virkar, T.B. Jackson and R.A. Cutler, J. Am. Ceram. Soc. 72 (1989) 2031-2042.
8. T.B. Jackson, A.V. Virkar, K.L. More and R.B. Dinwiddie, J. Am. Ceram. Soc. 80 (1997) 1421-1435.
9. C.H. Chu, C.P. Lin, S.B. Wen and Y.H. Shen, Ceram. Int. 35 (2009) 3455-3461.
10. X.L. Li, H.A. Ma, Y.J. Zheng, Y. Liu, G.H. Zuo, W.Q. Liu, J.G. Li and X. Jia, J. Alloys Compd. 463 (2008) 412-416.
11. X. He, F. Ye, H. Zhang and L. Liu, J. Alloys Compd. 482 (2009) 345-348.
12. L. Qiao, H. Zhou, H. Xue and S.H. Wang, J. Eur. Ceram. Soc. 23 (2003) 61-67.
13. Y. Kurokawa, K. Utsumi and H. Takamizawa, J. Am. Ceram. Soc. 71 (1988) 588-594.
14. T. Sakai and M. Iwata, J. Mater. Sci. 12 (1977) 1659-1665.
15. J.H. Enloe, R.W. Rice, J.W. Lau, R. Kumar and S.Y. Lee, J. Am. Ceram. Soc. 74 (1991) 2214-2219.
16. V.B. Shipilo, T.V. Rapinchuk, N.A. Shishonok, L.L. Sukhikh, T.S. Bartnitsksys and D.S. Yakovleva, Powder Metallurgy and Metal Ceramic, 32 (1993) 709-712.
17. A. Witek, M. Bockowski, A. Presz, M. Wroblewski, S. Krukowski, W. Wlosinski and K. Jablonski, J. Mater. Sci. 33 (1998) 3321-3324.
18. K. Watari, K. Ishizaki and T. Fujikawa, J. Mater. Sci. 27 (1992) 2627-2630.